

Experimental Study on Loop Heat Pipe Under Horizontal Condition With Different Working Fluids

Kyaw Zin Htoo^{†*}, Phuoc Hien Huynh[‡], Keishi Kariya^{††} and Akio Miyara^{††‡‡}

[†]Graduate School of Science and Engineering, Saga University 1 Honjo-machi, Saga, 840-8502, Japan

[‡]Ho Chi Minh City University of Technology – VNU – HCM (HCMUT) 268 Ly Thuong Kiet, Ho Chi Minh City, Vietnam

^{††}Department of Mechanical Engineering, Saga University 1 Honjo-machi, Saga, 840-8502, Japan

^{†††}International Institute for Carbon-Neutral Energy Research, Kyushu University Nishi-ku, Motoooka, Fukuoka, 819-0395, Japan

*Corresponding Author Email: kyawzinhtoo1992@gmail.com

ABSTRACT: Loop heat pipe (LHP), a naturally operated heat transfer device with exceptionally flexible and simple in construction, has been paid interest by many researchers and scientists. Additionally, the effectiveness of using LHP as a heat exchanging device can be seen by transmitting heat load at high rates over considerable distances with extremely small temperature drop. In this paper, instead of using the traditional method of the gravity-assisted orientation, the experiment is set up in horizontal condition. Water and ethanol are selected as two types of working fluids in this operation. Experimental results of horizontal orientation using water as a working fluid have already been reported. The present experimental set up is shown that the operation can be carried out a wider range of temperatures up to 124 °C at the surface of the heating block whereas the contribution of the previous set up is only up to 95 °C. For the comparison of the working fluids, the performance of the water LHP is by far superior to the ethanol. Unlike the ethanol LHP which have a stable, limited operation up to 57 W, the water LHP can be able to perform a considerable range of the heat load of 41 W to 244 W while the surface temperature of the heating block raised from 63 °C to 124 °C in the water LHP.

INTRODUCTION

Since being in demand of the electronic devices with smaller and more compacted designs, the amount of heat generated in such a small area is found to be in difficulty to dissipate by natural or forced convection. However, the establishment of the LHP by Gerasimov and Maydanik [1-3] in 1972, the idea of the application of LHP as a prime heat transfer device for the modern electronic devices has been receiving attention by many researchers and scientists. Besides, many studies have aimed to improve LHP performance and adapt to the needs of different working conditions. Kaya et al. [4] carried out experiments to study low power start-up characteristics with different orientations. The authors said that the required superheat, the maximum temperature at start-up, and the time required for start-up strongly depended on the loop orientation.

Pastukhov et al. [5-6] investigated miniature loop heat pipes with cylindrical evaporator less than 6 mm in diameter, and transport lines ranging from 1.5mm to 2mm in diameter. This LHPs designed for applications in electronics cooling. These loop heat pipes were able to hold power inputs up to 30W with heat transfer distances up to 0.25 m and used for cooling the central processing unit (CPU) of a mobile personal computer (PC). In their study, six different loop heat pipes with different sizes, sink designs, and wick materials are assembled, and working fluids are ammonia and acetone. The total thermal resistance from the source to the sink ranged from 1.4 °C/W to 4 °C/W by using an air-cooled heat sink. These loop heat pipes were examined successfully for a variety of orientation.

Moreover, LHP's performance is influenced by various factors that are properties of the working fluid, filling ratio, wick's characteristics, cooling and ambient condition, geometric designs of the component because of passive operating characteristics [7]. Therefore, it is required comprehensively to study the effect of LHP orientation on the heat transfer performance when the high heat flux is applied. On the previous study [8-9], the thermal performance of the loop heat pipe under gravity-assisted condition was investigated by using water and ethanol. While water LHP could operate as high the heat load as 535W for heater surface temperature 110°C, this temperature reached 133°C at 395W for ethanol LHP.

In this paper, an LHP with flat – rectangular evaporator is fabricated, and sintered stainless steel wick is used. The experimental condition is horizontally arranged. Water and ethanol are used as the two working fluids, and the experiment is operated by using the two different types of fluids one after another. In our previous test section [10], the connection between the compensation chamber and vapor collector of the evaporator makes the vapor trapped inside the compensation chamber easily, especially when

the LHP is operated under elevated temperature. As a result, the thermal performance of the LHP decreased. Therefore, a new test section was designed and fabricated by the Machinery Division at Saga University. The new design overcomes the above drawbacks by disconnecting the passage between the vapor collector and the compensation chamber so that the vapor has no chance of trapping inside the compensation chamber through the connection between the vapor collector and the compensation chamber which is existed in the previous design. Therefore, the vapor collector is completely separated from the compensation chamber despite the evaporator lid with or without being able to be fully covered.

Moreover, the new design allows the removal of the wick material easier than the previous design assemblies, shown in figure 1. The benefit of using the new model has been achieved by improving the performance with a considerable range of heat load with a higher range of temperature than the previous design method. [see ref: figure 4]

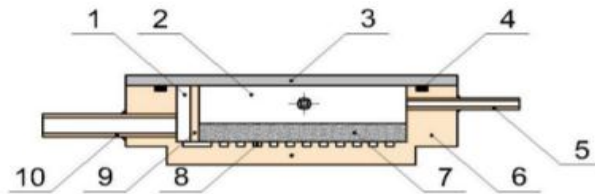


Figure 1. Schematic diagram of the previous evaporator 1: vapor collector; 2: compensation chamber; 3: poly carbonate lid; 4: O-ring; 5: charging pipe; 6: copper evaporator body; 7: wick; 8: vapor grooves; 9: copper plate; 10: vapor pipe.

EXPERIMENTAL APPARATUS AND DATA REDUCTION

Experimental Setup

The presented setup, which is shown in figure 2, is designed to investigate the performance under horizontal condition, using a copper-water closed two-phase loop heat pipe, for different heat loads.

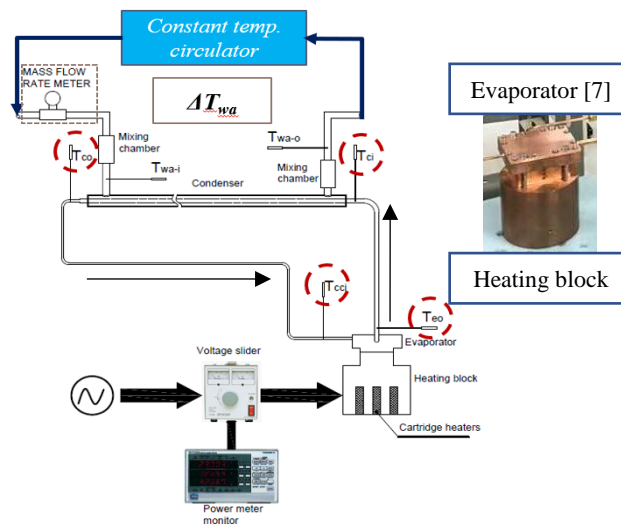


Figure 2. Schematic diagram of experimental setup

The evaporator is heated by four cartridge heaters installed inside the copper heating block. A thin layer of thermal conductivity grease is filled between heater and evaporator surface to minimize thermal contact resistance. Heat load is adjusted by the YAMABISHI MVS – 520 Volt slider and monitored on the YOKOGAWA WT230 digital power meter. On the other hand, the condenser is cooled by water whose inlet temperature is set at 28.5°C by the ADVANTEC LV – 400 constant temperature. The constant low-temperature circulator (ADVANTEC LV – 400) designed to provide a continuous supply of cooling water at a constant temperature and volume flow rate was used. From the flow direction of working fluids and cooling water, the condenser used in this loop heat pipe design can be classified as a double-pipe heat exchanger with counterflow arrangement.

To get a better understanding of the loop heat pipe and to determine the heat flux as well as evaporator base body temperature, thermocouples were distributed along the loop heat pipe as follows. Three 0.5mm-diameter K type thermocouples T_1 , T_2 , T_3 are inserted into the copper heating block and one 1mm-diameter K type T_4 in evaporator base body, as shown in figure 3.

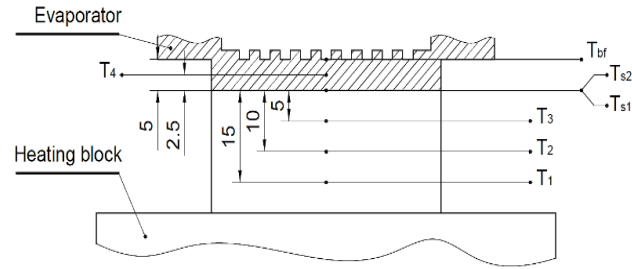


Figure 3. Temperature measurement inside heating block

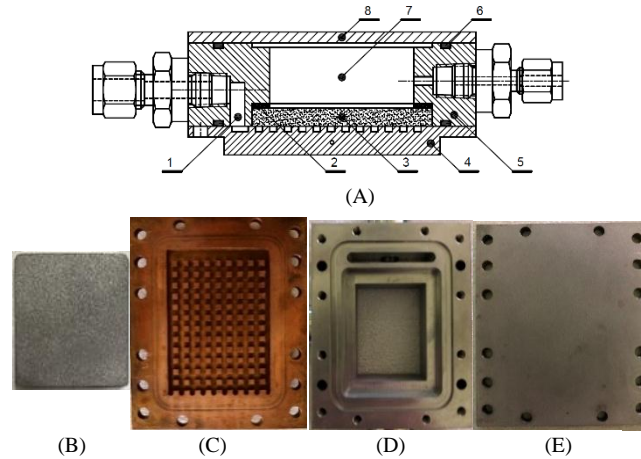


Figure 4. (A) Evaporator structure: vapor collector (1), silicone gasket (2), SS wick (3), copper base (4), SS body (5), O-ring (6), compensation chamber (7), SS lid (8); (B) Stainless steel sintered wick; (C) copper base of evaporator; (D) SS body; (E) SS lid

The temperature at the outlet of evaporator T_{eo} , inlet and outlet of condenser T_{ci} , T_{co} and inlet of compensation chamber T_{cci} are measured by four K type thermocouples inserted directly on the path of working fluid. Moreover, mass flow rate and temperature of cooling water at inlet and outlet are measured by MASSMAX MMM7150K mass flowmeters and two K type thermocouples. The experiment was carried out in the room with an air conditioner, and a control system was built. During the operation, room temperature is kept at 25 °C and observed by another K type thermocouple T_a . Except for the thermocouple T_a , all thermocouples are calibrated to sure that the uncertainty is ± 0.05 °C. A data acquisition system (Keithley 2071) was used to record the temperature measured throughout the experiment at a sampling rate of one data point per second for later analysis. The evaporator has the flat-rectangular shape to cool the electronics devices like processors as described in figure 4, which can contact well with the electronics surface. The evaporator consists of three main parts that are stainless-steel (SS) lid (8), copper base (4) and SS body (5), and the detailed specifications of the test loop are listed in table 1.

Table 1. The main parameters of LHP

Heating block	Copper
Mass, kg	4.36
Evaporator base	Copper
Length x Width x Height, mm	80 x 70 x 8
Active area, mm ²	60 x 45
Evaporator body	Stainless steel
Length x Width x Height, mm	80 x 70 x 23
Fin geometry	
Cross area, mm ²	2 x 2
Height, mm	1.5
Fin pitch, mm	4
Wick structure [11-12]	Stainless steel
Opening, μm	63

Void ratio, %	42
Bulk volume, mm ³	50 x 41 x 5
Compensation chamber	
Length x Width x Height, mm	40 x 31 x 18
Vapor line	Copper
OD/ID, mm	6.35/4.35
Length, mm	450
Condenser line	Copper
OD/ID, mm	6.35/4.35
Length, mm	300
Liquid line	Copper
OD/ID, mm	3.2/1.7
Length, mm	950
Working fluid amount (ml)	
Ethanol	31
Water	31

Experimental Condition and Charging System

During the experiment, the evaporator, the copper heating block, the condenser, the vapor and liquid transport lines were insulated. An array of fins or vapor crossing groove system was machined on the evaporator base to create the paths for vapor flow out evaporator as in figure 4, (C). With this design, no need to apply the unique fabricating technology to make the grooves on wick surface, but it promises enough space for evaporation, prevents vapor pocket forming inside the wicked body. The charging system in this experiment consists of a liquid stored tank, a liquid level indicator made of glass, control valves and a syringe, as shown in figure 5.

Firstly, mount the loop heat pipe to the charging system that is equipped with a high vacuum pump and evacuate the loop heat pipe from the non-condensable gases for 24 hours or until the vacuum pressure inside the system to remain constant. Secondly, introduce the working fluid charge into the charging system by using the syringe manually. In the second step, the loop heat pipe was disconnected by the control valve from the charging system.

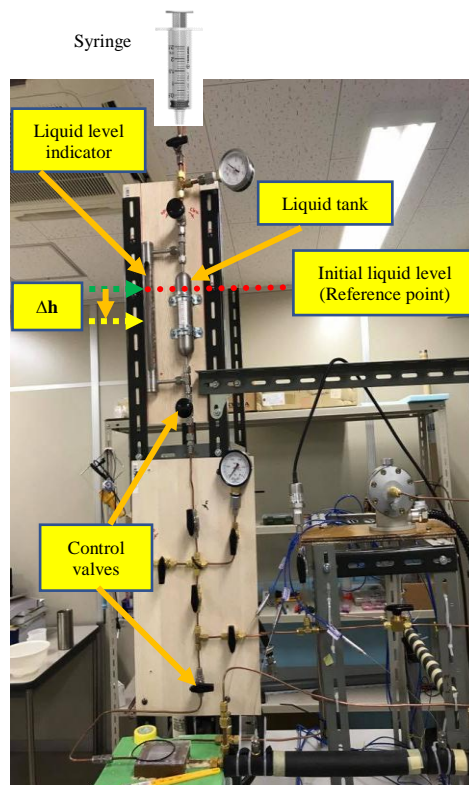


Figure 5. Photograph of experimental charging system

During this process, the vacuum condition of the charging system was lost; therefore, two experiments were run to determine the lowest pressure attainable. The first experiment was run using the vacuum pump only. The second experiment used a heat gun at various intervals to accelerate the removal of vapor. Finally, the control valves were used to add the working fluid into the loop heat pipe system, and the quantity of charged working fluid was determined from the liquid level indicator Δh . Moreover, the amount of the working fluid to charge the loop heat pipe was established by the following equations [13],

$$M = \rho_{l,h} [V_{liq} + V_{pw} + V_{sw} + (1 - \alpha)V_{cc}] + \rho_{v,h}(V_{gr} + V_{vap} + V_{con} + \alpha V_{cc}) \quad (1)$$

$$V_{pw} = Porosity \times V_{t,w} \quad (2)$$

$$\alpha = \frac{V_{v,cc}}{V_{cc}} \quad (3)$$

$$\Delta h = \frac{V_{lc}}{\frac{\pi D^2}{4}} \quad (4)$$

$$V_{lc} = \frac{M}{\rho_{lc}} \quad (5)$$

In this experiment, the parameter of α was set at 0.1, and the value of V_{sw} is neglected. Besides, the reference point of Δh is considered at the point which has the maximum diameter of the liquid tank. The purified water was also boiled and reduce the concentration of dissolved gases inside its volume before charged into the charging system. REFPROP 10.0 provided by NIST was used to obtain the density data. The temperature dependence of liquid and vapor density of water was considered in the calculation. By using the Pt100 thermometer (Chino Co. Model-R900-F25AT) as a standard source, measurement device uncertainties are listed in table 2.

Table 2. Uncertainty values of measurement devices

T_1, T_2, T_3	$\pm 0.06^\circ\text{C}$
T_4	$\pm 0.07^\circ\text{C}$
T_{eo}	$\pm 0.06^\circ\text{C}$
T_{co}, T_{cci}	$\pm 0.1^\circ\text{C}$
T_{wa-i}	$\pm 0.1^\circ\text{C}$
T_{wa-o}	$\pm 0.06^\circ\text{C}$
Mass flow meter	0.18% of reading

Data Reduction

The values of heat load Q and heat flux q flowing from the heating surface to the active area A (2700 mm^2) of evaporator were calculated by the following equations.

$$q = \frac{1}{3} \left(k \frac{T_1 - T_2}{\delta} + k \frac{T_2 - T_3}{\delta} + k \frac{T_1 - T_3}{2\delta} \right) \quad (6)$$

Where, $\delta = 5\text{mm}$.

$$Q = q * A \quad (7)$$

And the temperature of the heating block's top surface,

$$T_{s1} = \frac{1}{3} \left[\left(T_1 - 3 \frac{q\delta}{k} \right) + \left(T_2 - 2 \frac{q\delta}{k} \right) + \left(T_3 - \frac{q\delta}{k} \right) \right] \quad (8)$$

$$R_t = \frac{T_{s1} - T_{wa-i}}{Q} \quad (9)$$

Then, the total thermal resistance of the LHP can be calculated by the following equation.

RESULTS AND DISCUSSION

This section presents the results of experiments conducted on the LHP for cooling capacity and performance with two working fluids (water and ethanol) for various heat inputs. During the experiments, the condenser inlet temperatures T_{wai} of cooling water were maintained constant.

Operating Characteristics with Water and Ethanol as Working Fluid

The changes in the temperatures such as T_{s1} at the top surface of the heating block, temperatures at different positions in the LHP including T_{eo} , T_{ci} , T_{co} , and T_{cci} on the heating power when the LHP was charged with water and ethanol are demonstrated by following figures 6, 7, and 8. In this experiment, T_{s1} is regarded as the operating temperature of electronics like processors, and it is generally recommended that this temperature should not be higher than 85°C for reliable and safe performance [14].

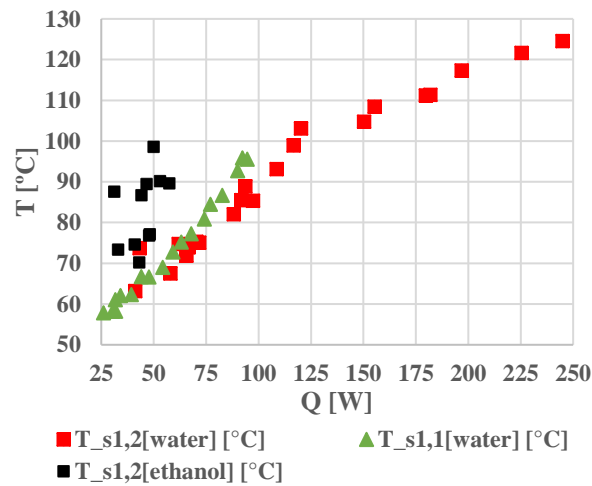


Figure 6. Temperatures T_{s1} varied with heat load, compared with the previous and new design evaporators

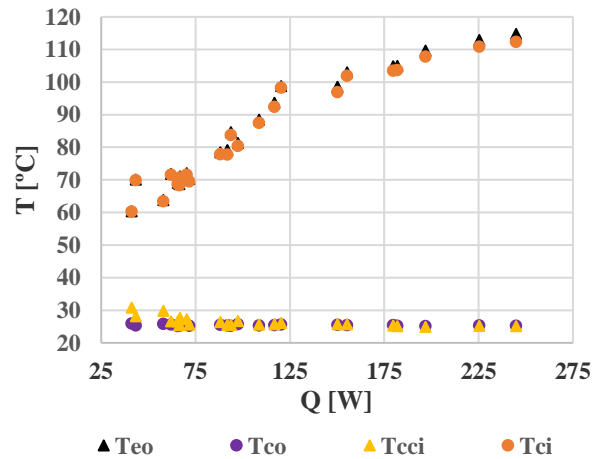


Figure 7. Temperatures at different locations vs heat load using water as the working fluid, using the new design evaporator

The results in figure 6 showed that the water LHP performed better than ethanol LHP. The water LHP could be operated stably in the range of 41 to 244 W, in which the temperature at the top surface of the heating block raised from 63°C to 124°C . In the case of ethanol, the stable operation was limited up to 57W, which is lower than water LHP. If a limited temperature of electronics is recognized at 85°C at the heater surface, the maximum heat load was 48 W for the ethanol LHP and 88 W for water LHP respectively. Moreover, the water LHP with the new evaporator design achieves the higher heat flux than the previous design of water LHP, while the ethanol LHP with the previous design could not make an operation.

Furthermore, as shown in figures 7 and 8, the temperatures T_{eo} and T_{ci} exist almost at the same values, while T_{co} and T_{cci} are nearly equal together. This result confirms working fluid circulates stably inside the loop for both water LHP and ethanol LHP. However, the ethanol LHP has higher fluctuations than the water LHP in the range of heat load from 31 W to 50 W, where the values of T_{cci} were slightly higher than the values of T_{co} . It means that the vapor-liquid interface near the thermocouple T_{cci} inside the liquid line appeared intermittently, and as a result, the supplying liquid for the compensation chamber could not flow stably. Therefore, the cooling performance of the condenser operating with ethanol was decreased, and the ethanol LHP could not operate as stably as the water LHP.

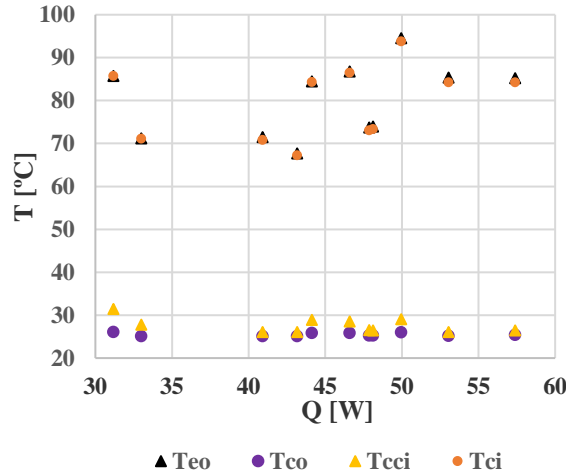


Figure 8. Temperatures at different locations vs heat load using ethanol as working fluid, using the new design evaporator

Changing of Total Thermal Resistance with Heat Load

Figures 9 and 10 present the total thermal resistance of the water LHP and ethanol LHP that are calculated by Eq. (9) and demonstrate that the water LHP operated better than ethanol LHP. In this experiment, the lowest thermal resistance was 0.4 K/W ($Q = 244$ W) for the water LHP with new evaporator design. In the case of ethanol LHP and water LHP with the previous design, they showed relatively high total thermal resistances such as 1.03 K/W and 0.7 K/W. The total thermal resistance of water LHP with the new and previous evaporator designs tend to decrease with the increasing heat input. When the supplied heat to the evaporator increased from 43 W to 244 W for the water LHP with the new evaporator design and from 26 W to 94 W for the water LHP with the previous design, the resistances were significantly reduced from 1.11 to 0.4 K/W and from 1.11 to 0.7 K/W for the previous design, respectively.

However, the cooling capacity of ethanol LHP was lower than the water LHP because of the higher thermal resistance existing at the condenser of the ethanol LHP. According to the thermal properties of water and ethanol, water has higher latent heat and liquid thermal conductivity. Therefore, the ethanol liquid condensing layer is thicker than the water at the same condition of heat released from the condenser and this liquid layer could become the resistance to prevent the heat transfer process from the vapor to cooling liquid. Besides, the condenser of water LHP could possess lower thermal resistance because of the low vapor density of water that makes vapor velocity higher. As a result, the total thermal resistance of the ethanol LHP reduced with the increased heating power only in the range of heat load from 31 to 43 W.

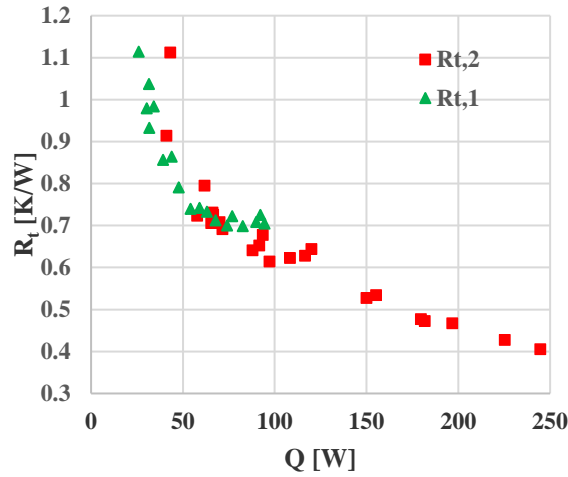


Figure 9. Total thermal resistance of the water LHP with the previous and new design evaporators

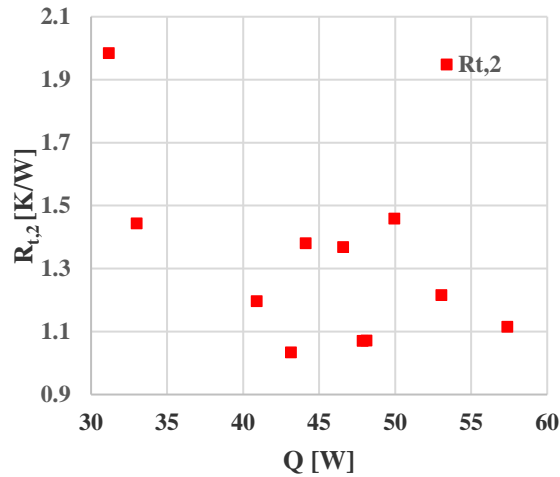


Figure 10. Total thermal resistance of the ethanol LHP with the new design evaporator

CONCLUSION

In this study, the LHP with the flat-rectangular evaporator was fabricated and investigated thermal performance under horizontal orientation with two working fluids (water and ethanol) for various heat inputs. Sintered stainless steel wick was installed inside the evaporator for the capillary pumping of them. The experimental results demonstrate that, the water LHP has better cooling performance than the ethanol LHP. The heater surface temperature of water LHP increased from 63 °C to 124 °C in the range of heat load from 41 to 244 W. In the case of ethanol, the stable operation was limited up to 57 W which is lower than water LHP. The water LHP could maintain the temperature at the top surface of the heating block smaller than 85°C when operating under heat power of 88 W. However, the ethanol LHP could satisfy this condition when the heat power was around 48 W only.

NOMENCLATURE

OD/ID	pipe outer, inner diameter, m
k	copper thermal conductivity, W/(m*K)
A	heating area, m ²

q	heat flux, W/m^2
Q	heating power, W
R_t	total thermal resistance, K/W
T_1, T_2, T_3	temperature inside the heating block, °C
T_4	temperature at the base of evaporator, °C
T_{bf}	temperature at the base of fin, °C
T_{ci}	temperature at the inlet of condenser, °C
T_{co}	temperature at the outlet of condenser, °C
T_{cci}	temperature at the inlet of compensation chamber, °C
T_{eo}	temperature at the outlet of evaporator, °C
T_{s1}	temperature at the top surface of the heating block, °C
T_{s2}	temperature at the evaporator bottom surface, °C
T_{wa-i}	temperature of the inlet cooling water, °C
T_{wa-o}	temperature of the outlet cooling water, °C
δ	distance among thermocouples T_1 , T_2 and T_3 , m
M	adequate charge amount, kg
V_{cc}	volume of compensation chamber, m^3
V_{vap}	volume of vapor line, m^3
V_{con}	volume of condenser, m^3

V_{liq}	volume of liquid line, m^3
V_{pw}	volume of primary wick, m^3
V_{sw}	volume of secondary wick, m^3
V_{gr}	volume of vapor groove, m^3
α	vapor ratio in compensation chamber
$\rho_{l,h}$	density of liquid in hot case, kg/m^3
$\rho_{v,h}$	density of vapor in hot case, kg/m^3
$V_{t,w}$	total volume of wick, m^3
$V_{v,cc}$	volume of vapor in compensation chamber, m^3
V_{lc}	volume of charged liquid, m^3
ρ_{lc}	density of charged liquid, kg/m^3
D	diameter of liquid tank, m
Δh	height difference in liquid level indicator, m

Subscripts

$(\)_{,1}$	LHP with the previous evaporator
$(\)_{,2}$	LHP with the new evaporator

REFERENCES

- [1] Heat Pipe, USSR Inventors Certificate 449213, 1974.
- [2] Yu. F. Gerasimov, Yu. F. Maydanik, G.T. Shchogolev, et al. "Low-temperature heat pipes with separate channels for vapor and liquid". *Eng.-Phys. J.* vol. 28, no. 6, pp. 957–960 (in Russian). 1975
- [3] Muhammad Ikram, A. Muhammad, A. Ur Rahmn, "Analytic Solution To Benjamin-Bona-Mahony Equation By Using Laplace Adomian Decomposition Method", *Matrix Science Mathematic*, vol. 3, no. 1, pp. 1-4, 2019.
- [4] T. Kaya, J. Ku, T.T. Hoang, and M. K. Cheung, 19993, "Investigation of Low Power Start-Up Characteristics of a Loop Heat Pipe". *Space Technology and Applications International Forum*, no.458, pp. 799-804, 1999.
- [5] V.G. Pastukhov, Y.F. Maydanik, C.V. Vershinin, and M.A. Korukov, "Miniature Loop Heat Pipes for Electronics Cooling". *Applied Thermal Engineering*, vol. 23, pp. 1125-1135, 2003.

- [6] K. Manoj, “Information and Communication Technology (ICT) and R&D for Innovation and Productivity”, *Advances In Industrial Engineering And Management*, vol. 8, no. 1, pp. 25-44, 2019.
- [7] S. Launay, V. Sartre, and J. Bonjour. “Parametric analysis of loop heat pipe operation: a literature review”. *International Journal of Thermal Sciences*, vol. 46, pp. 621–36, 2007.
- [8] P.H. Huynh, H.K. Zin, K. Kariya, A. Miyara: “Experimental Investigation Thermal Performance of Loop Heat Pipe Operating with Different Working Fluids”. *Journal of Advanced Thermal Science Research* (DOI: 10.15377/2409-5826.2019.06.3)
- [9] R. Kumar, “Comparison Of Instruction Scheduling And Register Allocation For MIPS And HPL-Pd Architecture For Exploitation Of Instruction Level Parallelism”, *Engineering Heritage Journal*, vol. 2, no. 2, pp. 4-8, 2018.
- [10] P.H. Huynh, A.R. Tuhin, K.Z. Htoo, K. Kariya and A. Miyara, “Experimental study on the loop heat pipe operating under horizontal orientation”. *Mechanical Engineering Research Journal*, vol.11, pp. 54-58, 2018.
- [11] SMC Coporation, Sinter metal element (EB/ES Series), pp. 103–11 [cited 2017 Nov. 27th]
- [12] S.K. Gugulothu, N.P. Kishore, V.P. Babu, G. Sapre, “CFD Analysis On Different Piston Bowl Geometries By Using Split Injection Techniques”, *Acta Mechanica Malaysia*, vol. 2, no. 1, pp. 23-28, 2019.
- [13] H. Nagano, E. Onogawa, F. Fukuyoshi, H. Ogawa, and H. Nagai (2010): “Effect of amount of fluid charge in thermal performance of loop heat pipe”. *Heat Transf. Res.*, vol. 39, no. 6.
- [14] K. Ebrahimi, G. F. Jones, and A. S. Fleischer (2014): “A review of data center cooling technology, operating conditions and the corresponding low-grade waste heat recovery opportunities”. *Renew. Sustain. Energy Rev.*, Vol.31, pp. 662-638.